Materials Science Forum Vols. 297-298 (1999) pp. 139-146

Shot-Noise Suppression in Nondegenerate Conductors

T. Gonzáles

Departamento de Física Aplicada, Universidad de Salamanca, Plaza de la Merced s/n,
ES-37008 Salamanca, Spain
E-Mail: tomasg@gugu.usal.es

Keywords: Shot-Noise Suppression, Mesoscopic Systems, Ballistic Transport, Diffusive Transport

Abstract. A microscopic analysis of shot-noise suppression in nondegenerate two-terminal conductors is reported. Calculations are performed by using a self-consistent semiclassical ensemble Monte Carlo simulation. Ballistic and diffusive transport regimes are analyzed. Different levels of suppression are obtained depending on the type of process controlling the current flowing through the device. Long-range Coulomb interaction is found to play an essential role in the shot-noise suppression provided significant space-charge effects take place inside the structures.

1 Introduction

Shot noise is caused by the randomness in the flux of carriers crossing the active region of a given device and is associated with the discreteness of the electric charge [1]. Uncorrelated carriers exhibiting Poissonian statistics are known to be characterized by a full shot-noise power given by the Schottky formula $S_I = 2qI$, with q the electron charge and I the d.c. current. However, correlations between carriers can reduce the noise, leading to suppressed shot noise, characterized by the expression $S_I = \gamma \cdot 2qI$, where $\gamma < 1$ is the suppression factor. Several interactions and mechanisms can introduce correlations among carriers, thus giving rise to different levels of suppression, which can constitute valuable information concerning the carrier kinetics inside the devices [2]. For this reason, the subject of shot-noise suppression in mesoscopic devices [3] is attracting increasing attention from both theoretical [4-12] and experimental points of view [13-17].

While most of the mechanisms introducing correlations between electrons have been extensively studied (Pauli principle, tunnelling, electron-electron interaction, etc.) [1,3], long-range Coulomb repulsion has received less attention. Its relevance to shot-noise suppression has been recognized since the times of vacuum tubes [18], however its role in modern mesoscopic structures, though claimed by several authors [2,10], is not yet quantitatively assessed. Furthermore, the controversy about the essential or marginal influence of coherent transport and degeneracy on the noise reduction is also of particular interest, especially in the case of diffusive conductors [2,4,5,9,12,19].

The aim of this work is to address the above problems. To this purpose, we review recent theoretical results on shot-noise suppression in *nondegenerate* mesoscopic samples, where a *semiclassical* transport model accounting for Coulomb interaction is considered. Calculations are based on an ensemble Monte Carlo (MC) simulation self-consistently coupled with a Poisson solver (PS). With this model we investigate shot-noise suppression and its frequency behaviour under the following conditions: (a) Ballistic transport regime, where the effects of long-range Coulomb interaction under different levels of space charge will be analyzed [11,20]. (b) Cross-over between ballistic and diffusive transport regimes under different carrier injecting statistics. (c) Diffusive transport regime. The last condition (c) is of relevant physical interest under both the cases of elastic and inelastic scattering. In the former case the universal 1/3 suppression factor [4,5,9,12], already evidenced experimentally [13,15,16], is found; in the latter case an even more pronounced suppression associated with energy dissipation [6-8,19] is evidenced. In both cases the role played by Coulomb interactions proves to be essential.

2 Physical model

For our analysis we consider the simple structure shown in Fig. 1. It consists of a lightly-doped semiconductor active region of length L sandwiched between two heavily-doped contacts which act as thermal reservoirs by injecting carriers into the active region. The structure is assumed to be sufficiently thick in transversal directions to allow a 1D electrostatic treatment. Accordingly, the MC simulation is 1D in real space and 3D in momentum space. The doping of the contacts n_c is always taken to be much higher than that of the active region N_D. Hence, when a voltage U is applied to the structure, all the potential drop is assumed to take place inside the active region between positions $x=0$ and $x=L$.

The modeling of carrier injection from the contacts is of crucial importance for the noise behaviour in mesoscopic devices. In our case, the contacts are considered to remain always at thermal equilibrium, and thus the velocity of the injected electrons follows a thermal-equilibrium Maxwell Boltzmann distribution at the lattice temperature T. On the other hand, the fluctuating injection rate is taken to follow a Poissonian statistics, i.e., the time between two consecutive electron injections is generated with a probability $P(t)=\Gamma e^{-\Gamma t}$, where $\Gamma=\frac{1}{2}n_c v_{th} S$ is the injection rate, $v_{th}=\sqrt{2k_B T/\pi m}$ the thermal velocity, S the cross sectional area of the device and m the electron effective mass [20]. This contact model is physically plausible and will be the one typically used. However, to analyze the influence of the contact injecting statistics on the noise behaviour, the following alternative models are also used: fixed velocity of the injected carriers in place of Maxwellian distribution, and uniform injection (at regular time intervals) in place of Poissonian statistics.

For the calculations we have considered a structure where L=200 nm, $T=300\ K$, $m=0.25m_0$ and $\varepsilon=11.7$ (relative dielectric contact). Several values of contact doping (and therefore several injection rates) from 10^{13} to 4×10^{17} cm^{-3} will be analyzed, thus leading to different levels of space-charge effects inside the active region, which will be characterized by the dimensionless parameter $\lambda=L/L_{Dc}$, with L_{Dc} the Debye length associated with the carrier concentration at the contacts. The values of λ will vary from very low values (0.15 for $n_c=10^{13}$ cm^{-3}), for which space-charge effects are negligible, to high values (30.9 for $n_c=4\times10^{17}$ cm^{-3}), where significant electrostatic screening takes place. Electrons move inside the active region following the classical equations of motion. Both ballistic and diffusive motion of carriers will be investigated. Elastic and inelastic (thermalizing) isotropic scattering mechanisms are introduced (separately) by means of an energy independent scattering time τ, whose value is appropriately varied (from 10^{-11} to 10^{-15} s) to cover both the ballistic and diffusive transport regimes. The transition between both regimes will be characterized by the ratio between the carrier mean free path ℓ (estimated as $v_{th}\tau$) and the sample length L. Static (*frozen* potential profile) and dynamic PS (potential profile updated at each time step) schemes will be used to evidence the influence of long-range Coulomb interaction on shot-noise suppression. Both schemes provide the same average current and steady-state spatial distributions of all the quantities, but the noise characteristics are in general quite different.

The structure operates under a constant applied bias. Under these conditions, the MC approach employed in the calculations allows the direct evaluation of the instantaneous fluctuating current [20]. The behaviour of the noise in the time domain is then determined by means of the autocorrelation function of current fluctuations, which, by Fourier transformation, provides the spectral density.

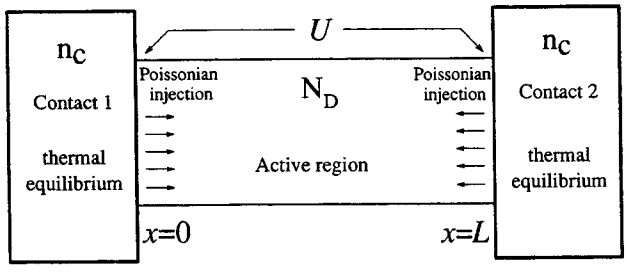

Fig. 1. Schematic drawing of the structure under analysis.

3 Results

In this section we present the results of shot-noise suppression corresponding to the different regimes of transport ranging from the ballistic to the diffusive ones.

A Ballistic regime. In this regime the carriers move in the active region of the structure without undergoing any scattering mechanism. Here the most peculiar characteristic is the existence of a minimum in the potential profile due to the presence of space charge. The amplitude of the minimum is larger at increasing λ (higher injection rate). At thermal equilibrium the minimum is located in the middle of the structure. When a positive voltage is applied to the anode (see inset of Fig. 2), the minimum is displaced toward the cathode, while its amplitude tends to decrease until vanishing at the highest voltages ($U > U_{sat}$), when the current in the structure saturates $I = I_S = q\Gamma$. This minimum constitutes a potential barrier for the electrons moving between the contacts. Thus, that part of electrons without enough energy to pass over the barrier are reflected back to the contacts. Furthermore, as carriers move through the active region, the dynamic fluctuations of the electric field (induced by long-range Coulomb interaction) modulate the transmission through the potential minimum and smooth out the current fluctuations imposed by the random injection at the contacts. As a consequence, the Poissonian statistics of the injected carriers is modified [21] and shot noise is suppressed [20]. This is illustrated in Fig. 2, where the low-frequency shot-noise suppression factor $\gamma = S_I(0)/2qI$, calculated with the dynamic PS, is shown as a function of the applied bias for several values of λ. Here, depending on the operating conditions, three different behaviours are identified in each curve, namely: (i) thermal noise, for $qU < k_BT$, when there is no suppression; (ii) suppressed shot-noise, for $k_BT < qU < qU_{sat}$, when shot noise is dominant and due to the effect of the potential barrier its level is reduced; and (iii) full shot noise, for $U > U_{sat}$, when the barrier controlling the current is washed out. Shot-noise reduction becomes more pronounced and covers a wider range of applied bias as λ increases (e.g. for λ=30.9, γ reaches a value of 0.045) due to the more significant space-charge effects. When a static PS is used, the potential profile is frozen, no interaction between carriers exists, and no suppression takes place [11].

To illustrate the time and frequency behaviour of the current fluctuations in the ballistic regime, in Fig. 3 we show the autocorrelation function $C_I(t)$ and the spectral density (inset) $S_I(f)$ calculated with the dynamic PS for the case of λ=7.72 at several voltages. Near equilibrium conditions the shape of the correlation function is determined by the contributions coming from two types of carriers: those which return to the contacts (*returning carriers*) and those which pass the potential

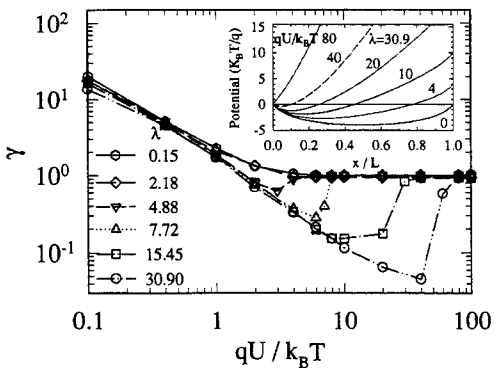

Fig. 2. Shot-noise suppression factor vs applied bias U for several values of λ. Inset: spatial profile of the potential for different applied voltages in the structure with λ=30.9.

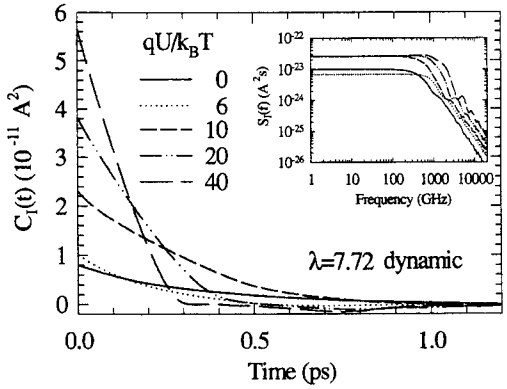

Fig. 3. Autocorrelation function and spectral density (inset) of current fluctuations calculated using the dynamic PS at several applied voltages.

barrier present in the structure (*passing carriers*) [20]. The former govern the behaviour of $C_I(t)$ at the shortest times, and the latter at the longest times. Starting from this shape near equilibrium, $C_I(t)$ tends to a triangular shape, more pronounced as the applied voltage increases. This triangular shape is typical of a constant-velocity emitter with all the electrons reaching the opposite contact [22]. In our case, electrons are injected at the cathode with a velocity which is Maxwellian distributed, but, due to the acceleration provided by the high electric field in the active region, the transit time of all carriers tends to become practically the same, its value decreasing at increasing applied voltages. Carriers injected at the anode immediately come back to the contact and thus play only an insignificant role at the shortest times. In the spectral density it can be observed that once saturation is reached ($qU > 8k_BT$) $S_I(0)$ takes the same value $2qI_S$ for all the applied voltages, but the spectra after the cut-off differ by showing smoothed *geometrical resonances* at different characteristic frequencies related to the corresponding transit times.

B Transition ballistic-diffusive regime. By introducing scattering mechanisms with decreasing characteristic time τ, we investigate the noise behaviour in the transition from ballistic to diffusive regime [23]. We analyze the influence of elastic and inelastic (thermalizing) scattering separately. In the following all the results correspond to the case of λ=30.9, which implies important space-charge effects inside the structure.

Fig. 4 shows the low-frequency spectral density of current fluctuations $S_I(0)$ normalized to $2qI_S$ as a function of ℓ / L for an applied voltage $U = 40\ k_BT / q$, calculated using static and dynamic PS. The evolution of the current in terms of $2qI$ is also shown. This evolution exhibits two limiting behaviours: (i) a first one ($\ell / L > 10^{-1}$) of saturation typical of ballistic or quasiballistic regime; (ii)

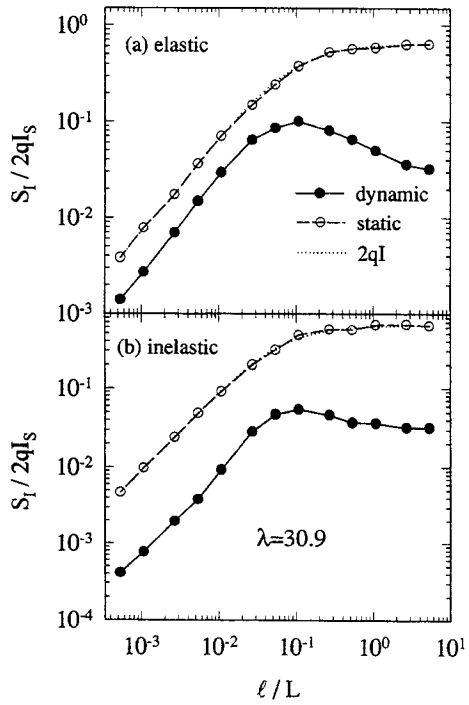

Fig. 4. Spectral density of current fluctuations (normalized to $2qI_S$) vs ballistic parameter ℓ/L for an applied bias U=40 k_BT/q, calculated with static and dynamic PS for the case of (a) elastic and (b) inelastic scattering.

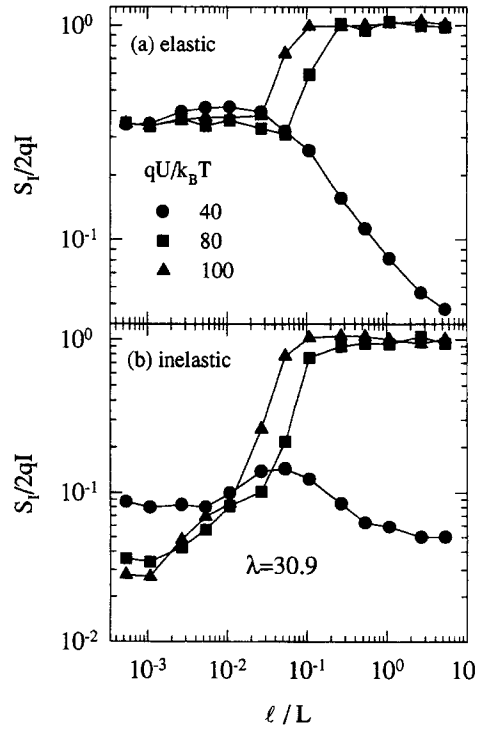

Fig. 5. Shot-noise suppression factor vs ballistic parameter ℓ/L for different applied voltages for the case of (a) elastic and (b) inelastic scattering. Calculations are performed by using dynamic potential.

and a second one ($\ell / L < 10^{-2}$) of linear decrease at decreasing ℓ / L typical of diffusive regime. Both in the elastic and inelastic cases $S_I(0)$ calculated with the static PS coincides exactly with $2qI$, thus revealing full shot-noise conditions when the dynamic fluctuations of the potential are ignored. On the contrary, with the dynamic PS $S_I(0)$ is systematically lower than $2qI$, thus evidencing a suppression effect. Here, in the ballistic limit elastic and inelastic cases present the same value, the suppression corresponding to that induced by the barrier fluctuations. As the diffusive regime is approached, the suppression remains active, being more pronounced in the inelastic case.

In Fig. 5 the suppression factor γ calculated with the dynamic potential is shown as a function of ℓ / L for several values of the applied voltage. The reason for the different behaviour found between the different curves in the ballistic limit is the presence or absence of the potential barrier related to the space charge. As compared with 40 $k_B T / q$, when the barrier is still present and the suppression is important, for the highest voltages (80 and 100 $k_B T / q$) the barrier has already disappeared, the current is saturated and the suppression factor takes on the full shot-noise level. In the elastic case, when the diffusive regime is achieved γ remains constant with ℓ / L and takes the same value of about 1/3 for all the applied voltages. On the contrary, in the inelastic case the higher the applied voltage, the lower the value of γ reached in the diffusive regime.

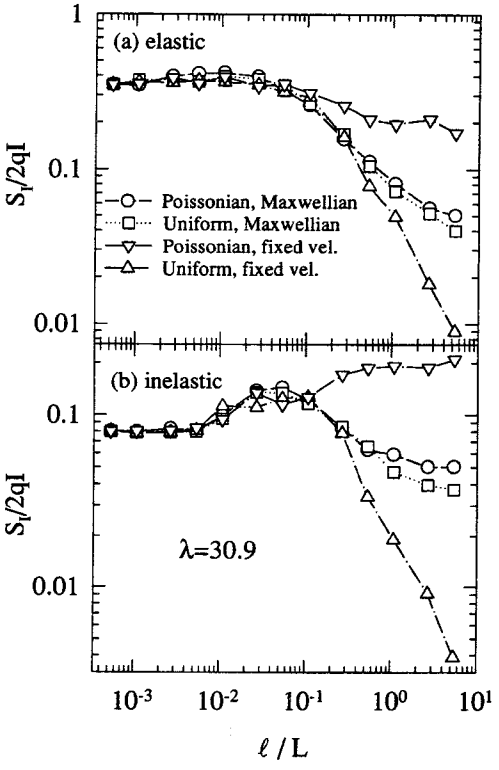

Fig. 6. Shot-noise suppression factor vs ballistic parameter ℓ/L for an applied bias U=40 k_BT/q and considering different contact models, calculated with dynamic PS for the case of (a) elastic and (b) inelastic scattering.

To check the influence of the contact injection on the evolution of the suppression factor with ℓ / L, Fig. 6 shows γ as a function of ℓ / L for an applied voltage of 40 $k_B T / q$ and for four different contact models, which combine Poissonian/uniform injection and Maxwellian/fixed-velocity distribution of the injected carriers. The Poissonian-Maxwellian injection is the one typically used. As expected, in the ballistic case, when the carrier transport in the structure is deterministic, the suppression factor crucially depends on the contact-injection model. For example, in the case of the uniform-fixed velocity contact, when the injection introduces no noise in the current flux, the suppression factor decreases drastically with the increase of ℓ / L, since the noise vanishes in the absence of scattering mechanisms. In diffusive regime, the results obtained with the four contact models are the same. This leads to the important conclusion that *the noise in the diffusive regime* (and particularly the 1/3 suppression factor obtained in the elastic-diffusive case) *is independent of the carrier injecting statistics*, and it is only determined by the effect of scattering mechanisms.

C Diffusive regime. In this section the results correspond to scattering times short enough to ensure diffusive transport in the sample (the ratio between the carrier mean free path ℓ and the length of the active region L is always lower than 3×10^{-3}).

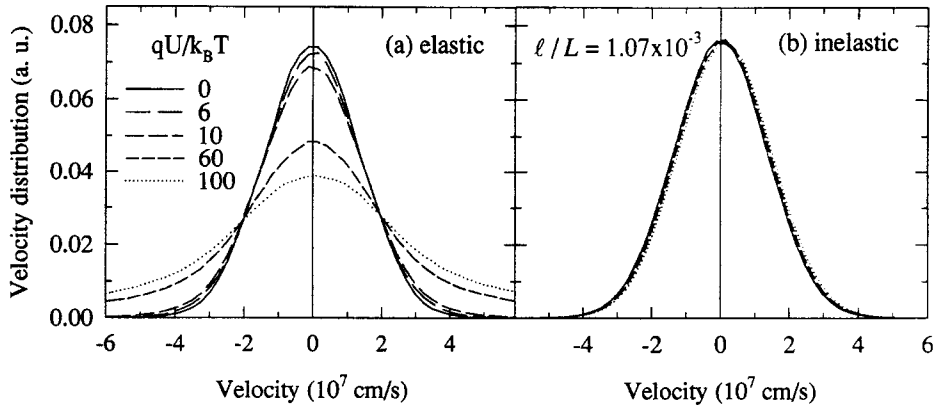

Fig. 7. Velocity distribution function of the carriers inside the active region of the structure with λ=30.9 for several applied voltages. (a) Elastic scattering, (b) inelastic scattering.

The behaviour of the noise in the diffusive regime is closely related to the breadth of the velocity distribution, which is shown in Fig. 7 for carriers inside the active region. In the elastic case, the distribution broadens when the applied voltage is increased, since there is no energy dissipation. In the inelastic case considered here, the energy is maximally dissipated, and a Maxwell-Boltzmann distribution at the lattice temperature T is obtained independently of the applied voltage. In both cases the distributions are very slightly displaced to positive velocities, as determined by the presence of a net current flowing through the structures.

Fig. 8 shows the dependence of the low-frequency suppression factor γ on the applied voltage U in both the elastic and inelastic cases calculated with the dynamic potential. In the inelastic case, according to the previous velocity distributions, the noise is just thermal Nyquist noise at any bias and, as a consequence, γ decreases systematically as the current increases (higher U). In the elastic case, at the lowest voltages the thermal behaviour is recovered; however, at the highest voltages, when the velocity distribution exhibits a strong deviation from equilibrium, the level of noise increases, its ratio with the current remaining constant and providing a value of 1/3 for the suppression factor γ. The results of the simulation are nicely reproduced by the expressions:

$$S_I^{inel} = 4k_BTG_0\frac{\langle N\rangle}{\langle N\rangle_0}, \qquad S_I^{el} = \frac{8}{3}k_BTG_0\frac{\langle N\rangle}{\langle N\rangle_0} + \frac{2}{3}qI\coth\left(\frac{qU}{2k_BT}\right), \tag{1}$$

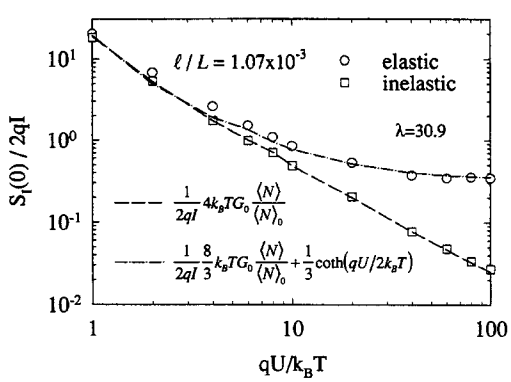

Fig. 8. Shot-noise suppression factor vs applied bias U calculated with dynamic potential for the cases of elastic and inelastic scattering mechanisms.

which correspond just to thermal noise (modulated by the variation in the number of carriers $\langle N\rangle$) in the inelastic case, and to the crossover from thermal ($qU << k_BT$, $S_I^{el} = 4k_BTG_0$) to suppressed shot noise ($qU >> k_BT$, $S_I^{el} = \frac{1}{3}2qI$) in the elastic case [5,9]. In these expressions k_B is Boltzmann constant, and G_0 and $\langle N\rangle_0$ the conductance and the average number of electrons inside the sample, both in the limit of vanishing bias.

The 1/3 value found in the elastic case for $qU >> k_BT$ is a well known *universal* result which has been obtained by very different theoretical approaches, going from the quantum-phase-coherent model of Beenakker and Büttiker

[4] to the semiclassical degenerate models of Nagaev [5] and de Jong and Beenakker [9]. In all these cases degenerate conditions are assumed, and the noise reduction comes from the regulation of electron motion by the exclusion principle. However, in our case neither phase-coherence [12] nor Fermi statistics are necessary for its appearance [19]. To explain the physical origin of the 1/3 value, Fig. 9 reports a typical frequency spectrum of the suppression factor under elastic-diffusive conditions for static and dynamic potentials. Here the current spectrum is decomposed into velocity, number, and cross-correlation contributions $S_I(f)=S_V(f)+S_N(f)+S_{VN}(f)$ [11]. In the static case the spectrum clearly shows that all three terms contribute to $S_I(f)$, and two different time scales can be identified. The longest one, associated with the transit time of the carriers through the device $\tau_T \cong 2$ ps, is evidenced in the terms $S_N(f)$ and $S_{VN}(f)$. The shortest one, related to the relaxation time of elastic scattering $\tau = 5$ fs, is manifested in $S_V(f)$. The latter term contributes with 1/3 to the full shot-noise value, while the former two terms provide the remaining 2/3. Thus, in the static case full shot-noise is recovered as sum of all three terms. On the contrary, in the dynamic case $S_N(f)$ and $S_{VN}(f)$ are found to exactly compensate each other and, as a result, $S_I(f)$ coincides with $S_V(f)$ in all the frequency range. It is interesting to notice that in the range between the transit and collision frequencies both static and dynamic suppression factors exhibit the 1/3 value, which is related to velocity fluctuations. However, at low frequencies only the dynamic case takes this value by virtue of Coulomb correlations, which are responsible for the mutual compensation of $S_N(f)$ and $S_{VN}(f)$ contributions. For this compensation to take place we have checked that it is necessary to fulfill the condition $L >> L_{Dc}$ in order to achieve a significant action of long-range Coulomb interaction. In addition, we have found that when a 2D momentum space is considered, the observed value of γ is about 1/2, which implies that the suppression factor is related to the dimensionality of momentum space.

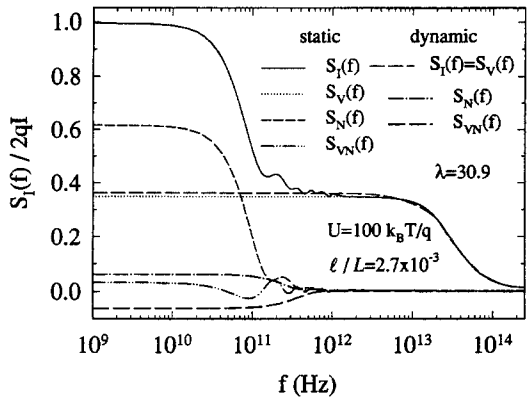

Fig. 9. Spectrum of the shot-noise suppression factor for the case of static and dynamic potentials under elastic diffusive conditions. Different contributions to the total value are shown in the figure.

4 Conclusions

Within an ensemble self-consistent MC scheme we have investigated the shot-noise suppression in nondegenerate conductors. The essential role played by long-range Coulomb interaction on the noise reduction has been demonstrated. Under ballistic regime, a sharp tendency of noise suppression at increasing values of space charge is found. Under diffusive regime, in the case of elastic scattering the universal 1/3 shot-noise suppression factor is obtained provided $qU >> k_BT$ and $L >> L_{Dc}$, and inelastic scattering is found to strongly suppress shot noise, reducing it to thermal Nyquist noise under heavily dissipative conditions.

Acknowledgements

The author gratefully acknowledges the contribution of several colleagues to this work: O.M. Bulashenko, C. González, J. Mateos, D. Pardo, L. Reggiani and J.M. Rubí. This work has been partially supported by the Comisión Interministerial de Ciencia y Tecnología through the project

TIC95-0652, the Dirección General de Enseñanza Superior e Investigación Científica through the project PB97-1331, and the Consejería de Educación y Cultura de la Junta de Castilla y León through the project SA11/96.

References

[1] Sh. Kogan: *Electronic Noise and Fluctuations in Solids* (Cambridge University Press, Cambridge 1996).

[2] R. Landauer: Physica B Vol. 227 (1996), pp. 156-160; Nature Vol. 392 (1998), pp. 658-659.

[3] M.J.M. de Jong and C.W.J. Beenakker: *Mesoscopic Electron Transport (NATO ASI Series E: Applied Sciences 345)*, ed L.L. Sohn *et al.* (Kluwer, Dordrecht 1997), pp. 225ff.

[4] C.W.J. Beenakker and M. Büttiker: Phys. Rev. B Vol. 46 (1992), pp. 1889-1892.

[5] K.E. Nagaev: Phys. Lett. A Vol. 169 (1992), pp. 103-107.

[6] A. Shimizu and M. Ueda: Phys. Rev. Lett. Vol. 69 (1992), pp. 1403-1406.

[7] R.C. Liu and Y. Yamamoto: Phys. Rev. B Vol. 50 (1994), pp. 17411-17414.

[8] K.E. Nagaev: Phys. Rev. B Vol. 52 (1995), pp. 4747-4743.

[9] M.J.M. de Jong and C.W.J. Beenakker: Phys. Rev. B Vol. (1995), pp. 16867-16870.

[10] M. Buttiker: *14th Int. Conf. on Noise in Physical Systems and 1/f Fluctuations*, ed. V. Bareikis and R. Katilius (World Scientific, Singapore 1995), pp. 35-40.

[11] T. González, O.M Bulashenko, J. Mateos, D. Pardo, and L. Reggiani: Phys. Rev. B Vol. 56 (1997), pp. 6424-6427.

[12] E.V. Shukorukov and D. Loss: Phys. Rev. Lett. Vol. 80 (1998), pp. 4959-4962.

[13] F. Liefrink, J.I. Dijkhuis, M.J.M. de jong, L.W. Molenkamp, and H. van Houten: Phys. Rev. B Vol. 49 (1994), pp. 14066-14069.

[14] M. Reznikov, M. Heiblum, H. Shtrikman, and D. Mahalu: Phys. Rev. Lett. Vol. 75 (1995), pp. 3340-3343.

[15] A.H. Steinbach, J.M. Martinis, and M.H. Devoret: Phys. Rev. Lett. Vol. 76 (1996), pp. 3806-3809.

[16] R.J. Schoelkopf, P.J. Burke, A.A. Kozhevnikov, D.E. Prober, and M.J. Rooks: Phys. Rev. Lett. Vol. 78 (1997), pp. 3370-3373.

[17] R.J. Schoelkopf, A.A. Kozhevnikov, D.E. Prober, and M.J. Rooks: Phys. Rev. Lett. Vol. 80 (1998), pp.2437-2440.

[18] B.J. Thompson, D.O. North, and W.A. Harris: RCA Rev. Vol. 4 (1940), pp. 269ff; RCA Rev. Vol. 4 (1940), pp. 441ff.

[19] T. González, C. González, J. Mateos, D. Pardo, L. Reggiani, O.M. Bulashenko, and J.M. Rubí: Phys. Rev. Lett. Vol. 80 (1998), pp. 2901-2904.

[20] T. González, J. Mateos, D. Pardo, O.M. Bulashenko, and L. Reggiani: Semicond. Sci. Technol. Vol. 13 (1998), pp-714-724.

[21] O.M. Bulashenko, J. Mateos, D. Pardo, T. González, L. Reggiani, and J.M. Rubí: Phys. Rev. B Vol. 57 (1998), pp. 1366-1369.

[22] T. Kuhn, L. Reggiani, and L. Varani: Superlatt. Microstruct. Vol. 11 (1992), pp. 205-209.

[23] T. González, O.M. Bulashenko, J. Mateos, D. Pardo, L. Reggiani, and J.M. Rubí: Semicond. Sci. Technol. Vol. 1053 (1997), pp. 1053-1056.